TWO DAYS NATIONAL LEVEL CONFERENCE

ON

ROLE OF PHYTOCHEMICALS AND ADVANCED MATERIALS IN CANCER PREVENTION AND RESEARCH

Sponsored By

TNSCHE

NGM COLLEGE

Chief Editor
Dr.K.Poonkodi

Joint Editors
Ms.K.Vimaladevi
Ms.R.Mini
Dr.V.Prabhu
Ms.M.Anusuya

PG DEPARTMENT OF CHEMISTRY
NGM COLLEGE, POLLACHI

INHIBITIVE ACTION OF HYDROXY PYRAZOLINE DERIVATIVES ON THE CORROSION OF MILD STEEL IN SULPHURIC ACID MEDIUM TOGETHER WITH QUANTUM CHEMICAL STUDIES

N.ANUSUYA[1], J SARANYA[2] and S.CHITRA[1*]

[1]Department of Chemistry, P.S.G.R. Krishnammal College for Women, Peelamedu, Coimbatore – 641004, Tamil Nadu, India.
[2]Department of Basic Science and Humanities, Gokaraju Rangaraju Institute of Engineering & Technology, Bachupally, Hyderabad - 500090

ABSTRACT

The corrosion inhibition properties of hydroxy pyrazoline derivatives for mild steel in 1 M sulphuric acid were studied using weight loss, potentiodynamic polarization and electrochemical impedance spectroscopic techniques. The effect of temperature on the corrosion behaviour of mild steel has been examined in the temperature range 303 – 333 K. The inhibition efficiency increases with increasing inhibitor concentration but decreases with increasing temperature. The adsorption of the inhibitors on mild steel surface obeyed the Langmuir adsorption isotherms. The density functional theory (DFT) at the B3LYP/6- 31G (d) basis set level was performed on hydroxy pyrazoline derivatives to investigate the correlation between molecular structure and the corresponding inhibition efficiency (%). The quantum chemical parameters such as E_{HOMO}, E_{LUMO}, the energy gap (ΔE), hardness (η), softness (S), dipole moment (μ), electron affinity (A), ionization potential (I), the absolute electronegativity (χ) and the fraction of electron transferred have been calculated.

Key words: hydroxy pyrazoline derivatives, mild steel, acid corrosion, Adsorption parameters DFT

INTRODUCTION

The environmental consequence of corrosion is enormous, and its inhibition has been deeply investigated. It has been found that one of the best methods of protecting metals against corrosion involves the use of inhibitors which are substances that slow down the rate of corrosion [1]. Therefore, the development of corrosion inhibitors based on organic compounds containing nitrogen, sulphur, and oxygen atoms is of growing interest in the field of corrosion and industry.

The corrosion and corrosion inhibition of iron in different environments have been reported in many research studies. Hydroxy pyrazoline derivatives have been reported to be effective inhibitors against corrosion of metals in corrosive media[2]. The objective of the present work is to study the inhibitive effect of synthesized hydroxy pyrazoline derivatives using gravimetric and electrochemical methods. To substantiate the experimental results, theoretical calculations were computed by applying density functional theory.

2. EXPERIMENTAL METHODS
### 2.1 Electrode Composition

Cold rolled mild steel specimen of size 1cm x 3cm x 0.08cm having composition 0.084% C, 0.369% Mn, 0.129% Si, 0.025% P, 0.027% S, 0.022% Cr, 0.011% Mo,

0.013% Ni and the reminder iron were used for weight loss measurements. For electrochemical studies, a mild steel rod of same composition with an exposed area of 0.785 cm^2 was used. The specimens were polished with 1/0, 2/0, 3/0 and 4/0 grades of emery sheets and degreased with trichloroethylene and dried using a drier. The plates were kept in a desiccator to avoid the absorption of moisture.

2.2 Synthesis of Inhibitors
2.2.1 Synthesis of hydroxy pyrazoline derivatives
The hydroxy pyrazoline derivatives were synthesized according to the reported procedure[3,4]. The molecular structures of the investigated compounds are as follows

Molecular structure of the inhibitors	
PNPM (II$_a$)	PPCT (II$_b$)
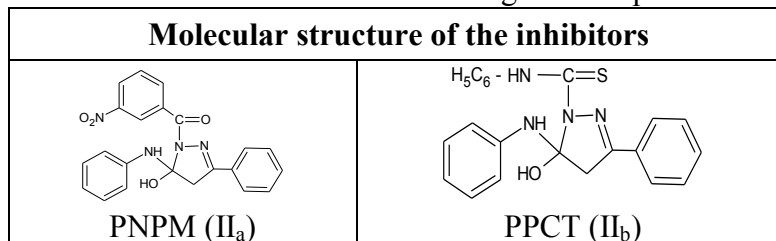
5-hydroxy-3-phenyl-5-(phenylamino)-4,5-dihydro-1*H*-pyrazol-1-yl](3-nitrophenyl)methanone (**PNPM**) II$_a$: Yield: 64%, Colour: brown, IR Spectrum (γ/cm^{-1}): 3205.83 (NH); 3274.31 (OH); 1739.64 (C=O)
5-hydroxy-N,3-diphenyl-5-(phenylamino)-4,5-dihydro-1*H*-pyrazole-1-carbothioamide (PPCT) II$_b$: Yield: 60%, Colour: brown, IR Spectrum (γ/cm^{-1}): 3259.84 (NH); 3293.59 (OH); 819.78 (C=S).

2.3 Weight loss method
The gravimetric method (weight loss) is probably the most widely used method for inhibition assessment. The initial weight of the polished specimen was taken. The solutions were taken in 100ml beakers and the specimens were suspended in triplicate into the solution using glass hooks. Care was taken to ensure the complete immersion of the specimen. After a period of three hours, the mild steel samples were taken out, washed with distilled water, dried and weighed to the accuracy of four decimals. From the initial and final mass of the specimen, (i.e before and after immersion in the solution) the loss in weight was calculated. The experiment was repeated for various concentrations of the synthesized inhibitors. The inhibition efficiency and corrosion rate were calculated from the weight loss results using the formulas,

$$Inhibition\ efficiency\ (\%) = \frac{W_b - W_i}{W_b} X100 \longrightarrow [1]$$

where, W_b = Weight loss without inhibitor; W_i= Weight loss with inhibitor.

$$Corrosion\ Rate\ (mpy) = \frac{534\ X\ Weight\ loss\ in\ g}{Density\ X\ Area\ (cm^2)\ X\ Time\ in\ hrs} \longrightarrow [2]$$

2.4 Electrochemical Techniques
The electrochemical impedance measurements were carried out for mild steel in acidic media using computer controlled potentiostat. (IVIUMCompactstat Potentiostat/Galvanostat). After immersion of the specimen prior to the impedance measurement, a stabilization period of 30 minutes was observed for E_{oc} to attain a stable value. The impedance measurements were made at corrosion potentials over a frequency

range of 10 KHz to 0.01Hz with a signal amplitude of 10mV. The real part (Z') and the imaginary part (Z'') were measured at various frequencies. A plot of Z' Vs Z'' were made. From the plot, the charge transfer resistance (R_t) and double layer capacitance (C_{dl}) were calculated.

$$In\Box ibition\ Efficiency\ (\%) = \frac{R_{t(inh)} - R_{t(blank)}}{R_{t(inh)}} x100 \longrightarrow [3]$$

where, $R_{t(inh)}$ = charge transfer resistance in the presence of inhibitor; $R_{t(blank)}$ = charge transfer resistance in the absence of inhibitor.

Polarization measurements were made after EIS studies in the same cell set up for a potential range of -200 mV to +200 mV with respect to open circuit potential at a sweep rate of 1mV/sec. From the plot, the inhibition efficiency, Tafel slopes corrosion potentials and corrosion current were calculated using IVIUM software.

$$In\Box ibition\ Efficiency\ (\%) = \frac{I_{corr(blank)} - I_{corr(in\Box)}}{I_{corr(blank)}} X100 \longrightarrow [4$$

where $I_{corr(blank)}$ and $I_{corr(in\Box)}$ are the corrosion current density values without and with inhibitors respectively.

2.5 Computational details

B3LYP, a version of the DFT method that uses Becke's three parameter functional (B3) and includes a mixture of HF with DFT exchange terms associated with the gradient corrected correlation functional of Lee, Yang and Parr (LYP)[5], was used to carry out quantum calculations. Full geometry optimization together with the vibrational analysis of the optimized structures of the inhibitor was carried out at the B3LYP/6-31G (d) level of theory using G03W program package. The quantum chemical parameters were calculated for molecules in aqueous form. It is well known that the phenomenon of electrochemical corrosion occurs in liquid phase. As a result, it is necessary to include the effect of a solvent in the computational calculations. In the G03W program, SCRF methods (Self-consistent reaction field) were used to perform calculations in aqueous solution.

Quantum chemical parameters such as the energy of the highest occupied molecular orbital (E_{HOMO}) and the energy of the lowest unoccupied molecular orbital (E_{LUMO}), the energy difference (ΔE) [$E_{HOMO} - E_{LUMO}$], the dipole moment (μ), hardness (η), softness (S), electrophilicity index (ω) and the fraction of the electrons transferred (ΔN) from the inhibitor to the metal surface (ΔN) and total energy (ΔT_E) were calculated at B3LYP/6-31G(d,p) level in aqueous phase. According to Koopman's theorem [6,7] the ionization potential (I) and electron affinity (A) Global hardness (η) [8] Global softness (σ) [8] of the inhibitors were calculated.Electronegativity (χ) [9]and the fraction of electrons transferred from the inhibitor to metallic surface, ΔN were also calculated.

3. RESULTS AND DISCUSSION
3.1Weight loss measurements

Weight loss of mild steel surface in 1M H_2SO_4 was determined at 303 - 333 K in the absence and presence of different concentrations of hydroxy pyrazolines (PNPM and PPCT). The obtained corrosion parameters are presented in Table 1 and 2. It is clear from the tables that the percentage inhibition efficiency increases with concentration of the

inhibitors and decreases with temperature. The increase in inhibition efficiency with increasing concentrations of the inhibitors at room temperature (303 K) is due to an increase in surface coverage resulting in retardation of the metal dissolution[10] .The efficiency of the inhibitor follows the order

PPCT > PNPM
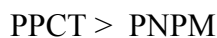
The maximum inhibition efficiency PPCT is may be due to the presence of the >C=S group[11]. According to **Every** and **Riggs**[12], organic compounds containing nitrogen and sulphur have better inhibition efficiency in acidic media compared to the organic compounds containing nitrogen or sulphur.

Effect of temperature

The results in Table 2 reveal that an increase in temperature decreases the inhibition efficiency. Generally, the metallic corrosion in acidic media is accompanied with evolution of hydrogen gas and rise in temperature usually accelerates the corrosion reactions resulting in higher dissolution rate of the metal[7]. A decrease in inhibition efficiency with temperature can be attributed to the increased desorption of inhibitor molecules from the metal surface or decreased adsorption process suggesting physical adsorption mode. But there are cases where chemical adsorption occurs, although inhibition efficiency decreases with increasing temperature[13].

3.2 Adsorption isotherm

Basic information on the interaction between the inhibitor molecules and the metal surface can be provided by the adsorption isotherm. The degree of surface coverage calculated from weight loss measurements corresponding to different concentrations of heterocyclic inhibitors were used to study the adsorption behaviour of heterocyclic inhibitors and to choose the more suitable adsorption isotherm. Attempts were made to fit the θ values to various isotherms including Langmuir, Temkin, El-Awadi and Flory-Huggins. The Langmuir adsorption isotherm was found to be best to describe the adsorption behaviour of the synthesized inhibitors on mild steel. The Langmuir isotherm is based on the assumption that all adsorption sites are equivalent and that particle binding occurs independently from nearby sites, whether occupied or not [14]. According to this isotherm, θ is related to C by:

$$\frac{C_{(inh)}}{\theta} = \frac{1}{K_{ads}} + C_{(inh)} \quad\quad\longrightarrow\quad [5]$$

where, K_{ads} is the equilibrium constant of the inhibitor adsorption-desorption process and $C_{(inh)}$ is the inhibitor concentrations. The plot of C/θ against inhibitor

concentration (C) at 303K and the expected linear relationship is obtained for all inhibitors with excellent correlation coefficient (r^2) (Table 3), confirming the validity of this approach. The slope values for all the inhibitors were found to be close to unity, suggesting that the adsorbed inhibitor molecules form a monolayer on the mild steel surface and there is no interaction among the adsorbed inhibitor molecules. Large values of K_{ads} obtained for all the inhibitors suggest strong adsorption and hence better corrosion inhibition efficiency. Using K_{ads} values the values of ΔG^{o}_{ads} were calculated by using the following equation.

$$\Delta G^{\circ}_{ads} = -RT \; ln \; (55.5 \; K_{ads}) \qquad \longrightarrow \qquad [6]$$

$$K = \frac{\theta}{C(1-\theta)} \qquad \longrightarrow \qquad [7]$$

where, θ is the degree of surface coverage on the metal surface, C is the concentration of inhibitor, R is gas constant and T is temperature. The negative values of (ΔG^{o}_{ads}) indicated the spontaneous adsorption of the inhibitors on the surface of mild steel [15]. The negative values of ΔG^{o}_{ads} ensure that the adsorption of the inhibitor molecule on to mild steel surface is a spontaneous process. Generally, values of ΔG^{o}_{ads} upto -20 kJ/mol are consistent with physisorption, while those around -40 kJ/mol or higher values are associated with chemisorption as a result of the sharing or transfer of electrons from organic molecules to the metal surface to form a coordinate type of metal bonds. In the present study, calculated values of ΔG^{o}_{ads} ranges between -22.41 and 29.29 kJ/mol suggest mixed mode of adsorption.

3.3 Electrochemical mesasurements
3.3.1 Potentiodynamic polarization measurements

Anodic and cathodic polarization curves for the corrosion of mild steel in 1M H_2SO_4 solution in the presence and absence of varying concentrations of inhibitors at 303K are shown in Figure 1. The corrosion current densities and corrosion potentials were calculated by extrapolation of linear parts of cathodic and anodic curves to the point of intersection. The electrochemical parameters such as corrosion potential (E_{corr}), corrosion current density (I_{corr}), anodic Tafel slope (b_a) and cathodic Tafel slope (b_c) and % IE determined from polarization curves are summarized in Table 4. The data in Table 4 clearly show that the current density decreases in the presence of inhibitors which indicates that inhibitors are adsorbed on the metal surface and hence the inhibition efficiency increased with the increase in the inhibitor concentrations. It is apparent from Table 4 that the values of b_a and b_c for all the studied inhibitors were found to change in the presence of inhibitors as compared to the values in the absence of the inhibitors (blank solution). Thus the addition of the inhibitors in blank solution affects both the anodic dissolution of steel and cathodic evolution of hydrogen. The variation in the values of anodic and the cathodic Tafel slopes in the presence of inhibitors suggest that the studied inhibitors are of mixed type[16]. However, the minor shift of E_{corr} values towards negative direction suggests the predominant cathodic control over the reaction.

3.3.2 Electrochemical Impedance Spectroscopy (EIS) Measurements

Electrochemical Impedance Spectroscopy analysis provide insight into the kinetics of electrode processes as well as the surface characteristics of the electrochemical system of interest. Fig 2 shows the Nyquist plots for mild steel in 1M H_2SO_4 in the absence and presence of different concentrations of heterocyclic derivatives at 303 K. The charge transfer resistance values (R_{ct}) are calculated from the difference in impedance at lower and higher frequencies, as described elsewhere [17]. To obtain the double layer capacitance (C_{dl}) the frequency at which the imaginary part of the impedance is a maximum, ($-Z_{i \; max}$) and C_{dl} values are calculated from the following equation :

$$C_{dl} = \frac{1}{2\pi \, R_{ct} \, f(-Z_i max)} \qquad\longrightarrow \qquad [8]$$

where $f(-Z_i \mathbf{max})$ is the frequency at which the imaginary part of the impedance is a maximum. Data in Table 5 showed that the inhibition efficiency increases by increasing the concentration of the studied inhibitors.The increase in the R_{ct} values is attributed to the formation of an insulating protective film at the metal solution interface. The decrease in C_{dl} values suggest a decrease in the local dielectric constant and/or an increase in the thickness of the electrical double layer, confirming the formation of a protective layer at the metal surface by the inhibitors. This type of behaviour can be generalized and explained by the Helmholtz model given in the following equation

$$C_{dl} = \frac{\varepsilon \varepsilon_0 A}{d} \qquad\longrightarrow\qquad [9]$$

where, ε is the dielectric constant of the medium, ε_0 is the permittivity of the free space, A is the effective surface area of the electrode and d is the thickness of the protective double layer formed by the inhibitors.

3.4 Quantum chemical study of the studied inhibitors in aqueous phase

Quantum chemical calculations have been widely used to study reaction mechanisms [18]. In this study, the relationship between quantum chemical parameters and inhibition efficiency was investigated. The frontier molecular orbital energies (*i.e.*, E_{HOMO} and E_{LUMO}) are significant parameters for the prediction of the reactivity of a chemical species. The E_{HOMO} is often associated with the electron donating ability of a molecule [19-21]. Therefore, increasing values of E_{HOMO} indicates higher tendency for the donation of electron(s) to the appropriate acceptor molecule with low energy and empty molecular orbital. According to Eddy and Ebenso [22], increasing values of E_{HOMO} facilitate the adsorption of the inhibitor. Consequently, the inhibition efficiency of the inhibitor would be enhanced by improving the transport process through the adsorbed layer. According to Table 6, the values of E_{HOMO} follow the order, PPCT > PNP, which is consistent with the experimental % inhibition efficiency results. However, the E_{LUMO} decreases in a similar order. This can be explained as follows. The E_{LUMO} indicates the ability of the molecule to accept electrons. Therefore, the lower the value of E_{LUMO} the more apparent it is that the molecule would accept electrons. Also, the $E_{LUMO-HOMO}$ (energy gap) was also found to decrease in the order similar to that of the E_{LUMO}. The data Table 6 show the energy gap for the studied inhibitors follow the trend PNP < PPCT, which confirms that PPCT is a best inhibitor. Literature reveals that a larger value of the energy gap indicates low reactivity to a chemical species because the energy gap is related to the softness or hardness of a molecule.

A soft molecule is more reactive than a hard molecule because a hard molecule has a larger energy gap [20,21].From Table 6, it is evident that the inhibitor with the least value of global hardness (hence the highest value of global softness) is the best and *vice versa*. This observation is consistent with the results obtained from experimental % inhibition efficiencies.

It is evident from the calculations that there is no obvious correlation between the values of the dipole moment with the trend of inhibition efficiency obtained experimentally. There is lack of agreement in the literature on the correlation between the

dipole moment and inhibition efficiency [22,24]. It may be concluded that physical adsorption results from electrostatic interaction between the charged centers of the molecules and charged metal surface, which results in a dipole interaction of molecule and metals surface. Therefore, the positive sign of the coefficient μ suggests that these inhibitors can be adsorbed on the mild steel surface by physical mechanism [25].

Values of ΔN show that the inhibition efficiency resulting from electron donation agrees with Lukovits's study [26]. If $\Delta N < 3.6$, the inhibition efficiency increases by increasing electron-donating ability of these inhibitors to donate electrons to the metal surface and it increases in the following order: PPCT > PNPM. The results indicate that ΔN values correlates strongly with experimental inhibition efficiencies. Thus, the highest fraction of electrons is associated with the best inhibitor (PPCT), while the least fraction is associated with the inhibitor that has the least inhibition efficiency (PNPM).The optimized geometries, HOMO and LUMO of the hydroxy pyrazoline derivatives (PPCT) in aqueous phase are presented in Table 7.

Table 1: Inhibition efficiencies of various concentrations of inhibitors for the corrosion of mild steel in 1M H_2SO_4 obtained by weight loss measurements at 303 K

Name of the inhibitor	Inhibitor con. (mM)	Weight loss (g)	Inhibition efficiency (%)	Corrosion rate (g cm^{-2} h^{-1})	Surface coverage (θ)
BLANK	-	0.2059	-	13.34	-
PNPM	0.5	0.1580	23.26	10.24	0.2326
	1.0	0.1415	31.28	9.17	0.3128
	2.5	0.1004	51.24	6.50	0.5124
	5.0	0.0767	62.75	4.97	0.6275
	7.5	0.0594	71.15	3.85	0.7115
	10.0	0.0396	80.77	2.57	0.8077
PPCT	0.5	0.0839	59.25	5.44	0.5925
	1.0	0.0465	77.42	3.01	0.7742
	2.5	0.0103	95.00	0.67	0.9500
	5.0	0.0071	96.55	0.46	0.9655
	7.5	0.0046	97.77	0.30	0.9777
	10.0	0.0019	99.08	0.12	0.9908

Table 2: Inhibition efficiencies at 10 mM concentration of inhibitors for the corrosion of mild steel in 1M H_2SO_4 obtained by weight loss measurements at higher temperatures

Name of the inhibitor	Temperature (K)	Weight loss (g)	Inhibition efficiency (%)	Corrosion rate (g cm^{-2} h^{-1})	Surface coverage (θ)
BLANK	303	0.0686	-	13.33	-
	313	0.1698	-	33.00	-
	323	0.282	-	54.81	-
	333	0.3927	-	76.32	-
PNPM	303	0.0132	80.76	2.57	0.8076
	313	0.0332	80.45	6.45	0.8045

	323	0.0665	76.42	12.92	0.7642
	333	0.0978	75.10	19.01	0.751
PPCT	303	0.0006	99.13	0.12	0.9913
	313	0.0029	98.29	0.56	0.9829
	323	0.0055	98.05	1.07	0.9805
	333	0.0119	96.97	2.31	0.9697

Table 3: Linear correlation coefficients and adsorption parameters for Langmuir relationship for the corrosion of mild steel in 1M H_2SO_4 at 303K

Name of the inhibitor	Slope	Linear coefficient regression (r^2)	K_{ads} (M^{-1})	$\Delta G^{\Box}_{ads}$ (KJ/mole)
PNPM	1.05	0.9959	2014.9	-29.29
PPCT	0.98	0.9997	290.61	-24.41

Table 4: Corrosion parameters for mild steel with selected concentrations of the inhibitors in 1M H_2SO_4 by potentiodyanamic polarization method

Name of the inhibitor	Inhibitor con. (mM)	Tafel slopes (mV dec^{-1})		E_{corr} (mV/SCE)	I_{corr} ($\mu A\ cm^{-2}$)	Inhibition efficiency (%)
		b_a	b_c			
BLANK	-	52	112	-472.4	1567	-
PNPM	0.5	66	133	-498.7	486.3	68.96
	5.0	52	158	-489.1	377.2	75.92
	10	60	150	-486.7	339.3	78.34
PPCT	0.5	70	130	-542.4	667.5	57.40
	5.0	34	145	-483.9	110.7	92.93
	10	38	209	-462.7	79.9	94.90

Table: 5 Electrochemical impedance parameters of mild steel corrosion in 1M H_2SO_4 for selected concentrations of the inhibitors

Name of the inhibitor	Inhibitor con. (mM)	R_{ct} (ohm cm^2)	C_{dl} ($\mu F\ cm^{-2}$)	Inhibition efficiency (%)
BLANK	-	11.06	36.6	-
PNPM	0.5	19.7	29.5	43.86
	5.0	33.6	26.5	67.08
	10	42.3	23.8	73.85
PPCT	0.5	52.1	20.6	78.77
	5.0	99.5	19.7	88.88
	10	151.1	16.3	92.68

Table 6: Calculated quantum chemical parameters for the inhibitors in the neutral form obtained using DFT at the B3LYP/6-31G (d) basis set in aqueous phase.

Name of the inhibitor	Total Energy (amu)	Dipole moment (μ)	E_{HOMO} (eV)	E_{LUMO} (eV)	ΔE, (eV)	Hardness (η)	Softness (σ)	ΔN
PNPM	-725.15	3.17	-6.220	-1.103	5.12	2.59	0.39	0.6524
PPCT	-705.54	5.07	-5.511	-1.307	4.19	2.09	0.48	0.8572

Table 7: The 3D-structure of synthesized inhibitors in the neutral form obtained using DFT at the B3LYP/6-31G (d) basis set in aqueous phase.
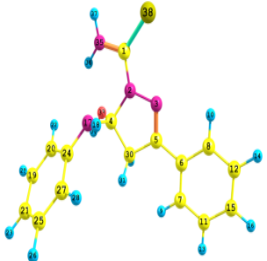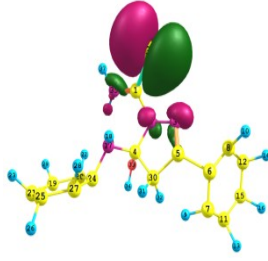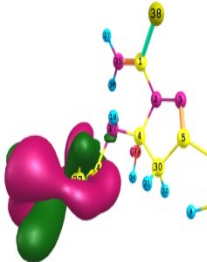
Name of the inhibitor	Optimized structure	HOMO	LUMO
PPCT			

Figure 1: Polarization curve for mild steel recorded in 1M H_2SO_4 for selected concentrations of inhibitor (PPCT)
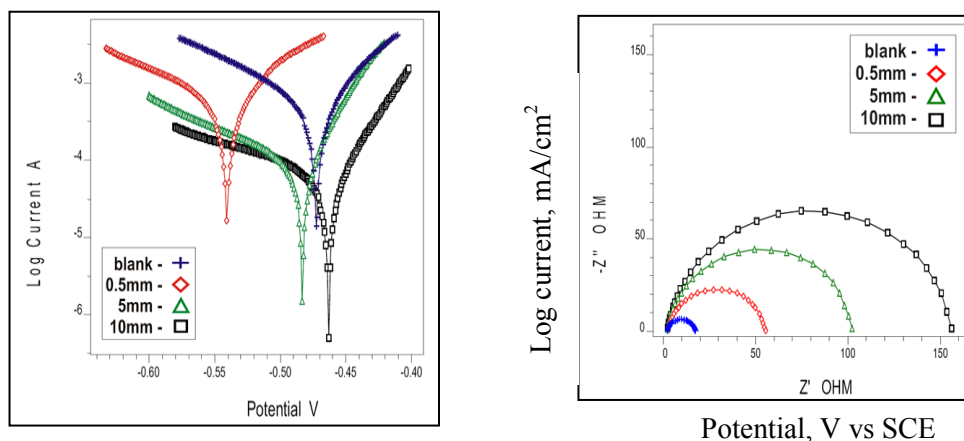

Figure 2: Nyquist diagram for mild steel in 1M H_2SO_4 for selected concentrations of inhibitor (PPCT)

CONCLUSIONS

- The high inhibitive effect of hydroxy pyrazoline derivatives are attributed to the adherent adsorption of the inhibitor molecules on the metal surface by formation of a protective film.
- Adsorption of the investigated hydroxy pyrazoline derivatives fitted Langmuir isotherm model.
- Polarization curves indicated that studied compounds behaved mainly as mixed inhibitor but predominantly cathodic in nature.
- Theoretical studies correlate with experimental results.

REFERENCES

1. K. Ajay Kumar, P. Jayaroopa, Int. J. Pharm. Tech., **5** (2013) 1473.
2. M.A. Amin, K.F. Khaled, Q.Mohren, H.A. Arida, , Corros. Sci. **52** (2010) 1684.
3. P.C. Sharma, S.V. Sharma, S. Jain, D. Singh, B. Suresh, Acta. Pol. Pharm., **66** (2009) 101.
4. S. Samshuddin, B. Narayana, B.K. Sarojini, R. Srinivasan, Vinayachandra, K.R. Chandrashekar, Der. Pharma. Chemica., **4** (2012) 587.
5. A.K. Chandra, M. T. Nguyen, Int. J. Mol. Sci. **3**(2002) 310.
6. P.Geerlings, F.De Proft, W. Langenaeker, Chem. Rev. 103 (2003) 1793.
7. R.G. Parr, R.G. Pearson, J. Am. Chem. Soc. **105** (1983) 7512.
8. L. Pauling, The nature of the chemical bond, Coruell University Press, Ithaca, New York, 1960.
9. Pearson R G, Inorg Chem,**27**(1988) 734.
10. S.A. Ali, A.M. El-Shareef, R.F. Al-Ghandi, M.T. Saeed, Corros. Sci., **47** (2005) 2659.
11. Y. Abboud, A. Abourriche, T. Saffaj, Desalination, **237** (2009) 175.
12. R.L. Every, O.L. Riggs, Mat. Prot., **3** (1964) 46.
13. A.Y. El-Etre, J. Colloid. interf. Sci., (2007) 578.
14. R. Solmaz, G. Kardas, M. Culha, B. Yazici, M.Erbil, Electrochim. Acta. **53**, (2008) 5941.
15. Shukla J, Pitre K.S, Corrosion Rev. **20**, (2002) 217.
16. D. Jayaperumal, Mater.Chem. Phy. **119** (2010) 478.
17. S.S. Abdel-Rehim, Magdy A.M. Ibrahim, K.F. Khaled, J. Appl. Electrochem., **29**, (1999) 593.
18. I.L. Rosenfeld, Corrosion Inhibitors, McGraw-Hill, New York, 1981.
19. S. Xia, M. Qiu, L.Yu, F. Liu, H. Zhao, Corros. Sci. **50** (2008) 2021.
20. E. E.Ebenso, T. Arslan, F. Kandemirli, N. Caner, I. Love, Int. J. Quantum Chem. **110** (2010) 1003.
21. T. Arslan, F. Kandemirli, E.E. Ebenso, I. Love, H. Alemu,Corros. Sci. **51** (2009) 35.
22. N. O. Eddy, E. E. Ebenso, J. Mol. Model. (2010), doi:10.1007/S00894-0090635-6.
23. L. M. Rodrigez-Valdez, A. Martinez-Villfane, D. Glossman-Mitnik, *J.* Mol. Struct. (THEOCHEM) **713** (2005) 65.
24. A.Stoyanova, G. Petkova, S.D. Peyerimhoff, Chem. Phys. **279** (2002) 1.
25. K.F. Khaled, M.M. Al-Qahtani, Mater.Chem.Phys. **48** (2003) 2635.
26. I.Lukovits, E. Kalman, F. Zucchi, Corrosion,(NACE) **57** (2001) 3.